Failure Propensity of GFRP Strengthen RC Beam

Anjani Kumar Shukla, Prateek Goswami & Pabitra Ranjan Maiti

Journal of Failure Analysis and Prevention

ISSN 1547-7029
Volume 20
Number 4

J Fail. Anal. and Preven. (2020)
20:1308-1322
DOI 10.1007/s11668-020-00939-1

Springer

J Fail. Anal. and Preven. (2020) 20:1308–1322
https://doi.org/10.1007/s11668-020-00939-1

TECHNICAL ARTICLE—PEER-REVIEWED

Failure Propensity of GFRP Strengthen RC Beam

Anjani Kumar Shukla · Prateek Goswami · Pabitra Ranjan Maiti

Submitted: 20 June 2020 / Published online: 4 August 2020

Abstract Fiber-reinforced polymer has eventually become a popular choice for retrofitting and strengthening of structural entities. Hence, a need arises to know the quantitative as well as qualitative effect of these techniques on the original integrity of the concerned structural entity. In the present study, the effect of change in width to depth ratio, percentage of steel and loading intensity in a simply supported reinforced concrete (RC) beam on the maximum deflection, stress, strain energy, natural frequencies and deflections of various modes of free vibration is obtained with the help of ANSYS Workbench 19.0 software till the failure of RC beam and a comparison is sought between the original beam and a failed beam retrofitted with one, two and three layers of GFRP sheets (Epoxy S-Glass UD). A standard beam of fixed dimensions and a two point loading was first simulated in the software while comparing the results with the manual calculations of maximum deflections to ascertain the most appropriate settings of the simulation in the three dimensional analysis environment of the software. Various beams were then analyzed altering the width to depth ratio, the percentage of tension steel and the loading intensity over the beam and the results of the static as well as modal (frequency) analysis were noted including the deflections, stresses, strains, strain energies, natural frequencies of first 5 modes of free vibrations and their respective displacements. The same beams were then retrofitted with layers of GFRP sheets with their principal axis inclined at an angle of 45° with the span of the beam. The same analysis was done on the beams and the results were noted. These results are compared, and a multivariate regression analysis is performed over the results to obtain equations to testify the observations and the trends. This whole process gives a conclusion that the effect of retrofitting is insignificant for single layer GFRP while the most effective results were obtained for the case of triple layer GFRP. Deflections, stress and strain energy with their relative change across various cases are accurately related to the varying parameters through regression analysis. Frequency is also accurately related but the relative change in frequency is not well established.

Keywords Failure analysis · GFRP · Reinforced concrete beams · Retrofitting · Multivariate regression analysis · Finite element analysis

A. K. Shukla (✉) · P. R. Maiti
Indian Institute of Technology (BHU) Varanasi, Varanasi, UP, India
e-mail: akshukla.rs.civ16@iitbhu.ac.in; er.anjanishukla@gmail.com

P. Goswami
Motilal Nehru National Institute of Technology Prayagraj, Allahabad, UP, India
e-mail: prateekgo999@gmail.com

Introduction

Concrete is the second most consumed product after water on earth and certainly Reinforced Cement Concrete (RCC) comprises a majority of that consumption. A vast majority of the civil engineering structures that are being built today or have been built in the past 100 years have concrete as the dominant building material and hence these have been or will be subjected to the ravishes of time and nature. As concrete ages, it strengthens but deteriorates in a corrosive environment. RC structures encounter damage even before the expiry of their service life due to many reasons like earthquakes, improper construction techniques, inefficient

design, explosions, fires, change of usage, corrosion, floods, etc. Hence, they call for immediate damage detection and a check for their integrity to estimate the remaining life span of the structure and the extent of serviceability that can be expected from the structure. These measures also aid in determining the suitable mitigation measure to increase the remaining life and enhance the integrity of the structure. The reinforced concrete structure fails in the brittle manner if the GFRP is below 0.5% of total reinforcement area, while increasing the area of GFRP from 0.5 to 1.0% results in the increment of ultimate load taking capacity with 67% and energy absorption capacity with 48 and 27% decrement in the mid span deflection [1]. When the GFRP sheet layers are placed at the bottom of the slab, then the displacement of slab got reduced [2]. It has been experimentally verified that the use of GFRP sheet at the spalling area of concrete improve the ultimate load capacity of infected area and also decrease the deflection at that point [3]. The analytical analysis of repaired bridge with jacketing at bottom of the slab decreases the stress in the tension zone of slab with better vibration absorption capacity [4]. The combination of steel cage and GFRP in the repairing of RC structures gives the confinement to the damaged members and prevents the joints of structures from excessive distortion [5]. Near surface mounted GFRP rods reduce the changes in the values of frequencies of the structures, and the failure of RC beam strengthen using this techniques depends on the bonding of RC beam and GFRP [6].

Pre-damage rehabilitation/strengthening are known as retrofitting while post-damage is called repairing. FRP (Fiber-Reinforced Plastics) has emerged as a popular retrofitting material recently and FRP plates as an application of the plate bonding methods are quite reliable. The FRPs employed in construction industry are mainly of three types [7] viz. glass fiber-reinforced plastics (GFRPs), carbon fiber-reinforced plastics (CFRPs), aramid fiber-reinforced plastics (AFRPs).

RC beams strengthened with FRPs suffer failure in three ways, i.e., flexure, shear and de-bonding with the de-bonding of the FRP sheet being the dominant failure mechanism. The plates can be provided on the tension side of the beams to enhance flexural strength and on the lateral sides to enhance its shear resisting properties as shown in Fig. 1.

Studies have shown that FRP confined concrete behaves differently from steel confinement due to the linear elastic properties of FRP up to failure [8]. Steel plates and FRP sheets together have been used to increase the efficiency of retrofitting [9]. Comparatively, FRP materials are more expensive but advantageous in overall economy, speed of retrofitting and ease of installation especially in places difficult to reach. In addition to that FRP sheets can be employed over a wide range of structural entities like beams, columns, connections, floors, girders, etc. Use of CFRP layers on columns have been found to increase the maximum load it can sustain by about 27%.While using it with GFRP bars have increased these numbers to 51% [10]. Use of these techniques has also affected the method of failure from flexure-shear failure to plastic hinging in some cases. Another study conducted on low strength concrete beams has shown an increase of 19–27(%) in strength depending on the configuration of CFRP pile sheets used in retrofitting [11].

There are significant numbers of studies on the static performances of the structural entities but not many incorporate the modal analysis and effect of these techniques on the natural frequencies and mode shapes of a structure. The knowledge of natural vibrations of a structure is indispensable today for seismic design. In 1985 Mexico City earthquake, most buildings that were damaged were between 6 and 15 stories, which collapsed as their natural mode of vibration was close to that of the earthquake. Hence, a study of the effect of retrofitting on these properties of the structure is essentially required.

Objective

The objective of the present study is to quantify the effect of retrofitting by GFRP jacketing for flexure on the static and modal behavior of a simply supported beam. For this purpose both static structural analysis and modal analysis are performed on different variations of the same beam in a 3D simulation environment of ANSYS Workbench 19.0.

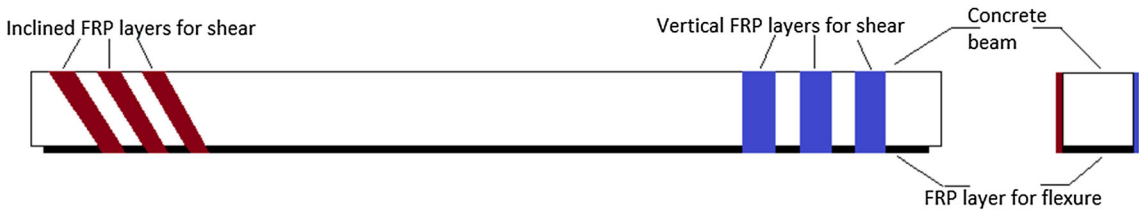

Fig. 1 Plan of RC beam retrofitting using GFRP

This software uses FEA (Finite Element Analysis) to analyze complex real world problems by simulating the same virtually [12]. For this study, about 90 beam models were simulated to generate a wide array of data. These data are further used to come up with the relevant trends and relations with the aid of graphs and statistical techniques.

Mechanical Properties of Materials

Mathematical Background

A beam is selected as a benchmark and it is analyzed analytically. The same beam is simulated in ANSYS and the results are compared to verify that the simulation is correct. The methods used are described in "Verification of analysis" and "Different cases of beams" sections.

Analytical Approach

Manually, the deflection is calculated by transformed area approach for uncracked section [13]. Uncracked section immediately on loading can be analyzed by applying the concept of modular ratio $n = E_s/E_c$, where E_s is the modulus of elasticity of steel and E_c is the modulus of elasticity of concrete. In Fig. 2 A_s is area of tension steel and A'_s is area of compression steel.

For an uncracked section subjected to a bending moment M, Fig. 2 shows transformed section, strain distributions and stress distributions.

$$\varepsilon_u = \frac{f_u}{E_c} = \frac{Myh}{E_c I_u}$$

where h is the total depth (thickness) of the section, f_u is extreme fiber compression stress in concrete, y is the ratio of the neutral axis depth to the total depth (thickness) and I_u is the moment of inertia of the uncracked transformed section.

Stresses in concrete at different fibers of uncracked section can be calculated directly by using the properties of corresponding transformed section and the bending equation of elastic homogenous beam. For reinforcing steel, the stress will be a product of modular ratio and the stress in transformed section at the same level.

The deflection is calculated by the Macaulay's method. The starting point is the relation from Euler–Bernoulli beam theory

$$\frac{d^2v}{dx^2} = \frac{M}{E_c I_u}$$

where v is the deflection and M is the bending moment as a function of x. For general loadings, M can be expressed in the form;

$$M = M_1(x) + P_1\langle x - a_1\rangle + P_2\langle x - a_2\rangle + P_3\langle x - a_3\rangle + \cdots.$$

where the quantities $P_i\langle x - a_i\rangle$ represents the bending moment due to point loads and the quantity $\langle x - a_i\rangle$ is a Macaulay bracket defined as:

$$\langle x - a_i\rangle = \begin{cases} 0 & \text{if } x < a_i \\ x - a_i & \text{if } x > a_i \end{cases}$$

and $\int P\langle x - a\rangle dx = P\frac{\langle x-a\rangle^2}{2} + C_m$

Numerical Approach

ANSYS uses finite element analysis to solve the problems input. Finite element analysis employs numerical methods to approximate the solutions of mathematical problems that are usually formulated so as to state an idea of physical reality. Most of these problems are described by partial differential equations and it is quite difficult to solve these equations at once. To make simulations, a mesh, consisting of up to a million of small elements that form the shape of the structure needs to be created. Every single element is calculated upon and the individual results are combined to give the final result of the structure is shown in Table 1.

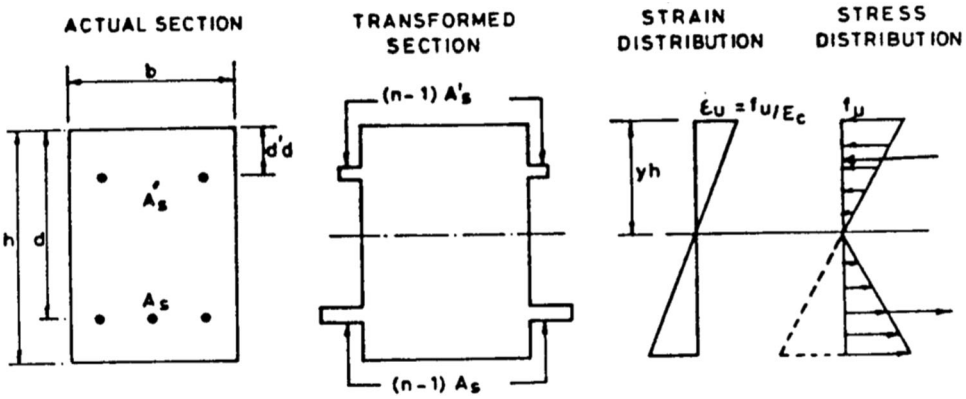

Fig. 2 Uncracked section

Table 1 Mechanical properties of Epoxy S-Glass UD (ANSYS material library)

S. no.	Property	Value	Unit
1	Density	0.000000002	mm^{-3t}
2	Young's modulus *X*-direction	50000	MPa
3	Young's modulus *Y*-direction	8000	MPa
4	Young's modulus *Z*-direction	8000	MPa
5	Poisson's ratio *XY*	0.3	NA
6	Poisson's ratio *YZ*	0.4	NA
7	Poisson's ratio *XZ*	0.3	NA
8	Shear modulus *XY*	5000	MPa
9	Shear modulus *YZ*	3846.2	MPa
10	Shear modulus *XZ*	5000	MPa
11	Tensile stress in *X* direction	1700	Mpa
12	Tensile stress in *Y* direction	35	Mpa
13	Tensile stress in *Z* direction	35	Mpa
14	Compressive stress in *X* direction	− 1000	MPa
15	Compressive stress in *y* direction	− 120	MPa
16	Compressive stress in *z* direction	− 120	MPa
17	Shear stress *XY*	80	MPa
18	Shear stress *YZ*	46.154	MPa
19	Shear stress *XZ*	80	MPa
20	Tensile strain in *X* direction	0.0244	NA
21	Tensile strain in *y* direction	0.0035	NA
22	Tensile strain in *z* direction	0.0035	NA
23	Compressive strain in *X* direction	− 0.015	NA
24	Compressive strain in *Y* direction	− 0.012	NA
25	Compressive strain in *Z* direction	− 0.012	NA
26	Shear strain *XY*	0.016	NA
27	Shear strain *YZ*	0.012	NA
28	Shear strain *XZ*	0.016	NA

Static Analysis

For static structural analysis of the structure linear perturbation theory is employed. It comprises mathematical methods to find an approximate solution to a problem, starting from the exact solution of a related, simpler problem. This theory is applicable if the problem at hand cannot be solved exactly, but can be formulated by adding a small term to the mathematical description of the exactly solvable problem. This leads to an expression of the desired solution A in terms of a power series known as perturbation series:

$$A = A_o + \varepsilon^1 A_1 + \varepsilon^2 A_2 + \cdots$$

here A_o is the known solution to the exactly solvable initial problem and A_1, A_2… are the higher order terms which may be found iteratively by some systematic procedure. As ε becomes small these higher order terms also become successively smaller. The approximate linear perturbation solution is obtained by truncating the series as:

$$A \approx A_o + \varepsilon A_1$$

Frequency Analysis

The modal analysis of the beam is performed by solving the classical eigenvalue problem:

$$[K]\{\phi_i\} = \omega_i^2[M]\{\phi_i\}$$

where $[K]$ = Stiffness matrix, $\{\phi_i\}$ = Mode shape vector (eigenvector) of mode i, Ω_i = Natural circular frequency of mode i (ω_i^2 is the eigenvalue), $[M]$ = Mass matrix

The numerical method used for solving this problem is the Block Lanczos mode extraction method. It consists of a set of Lanczos "runs", in which a set of iterations are performed. For each Lanczos run, the following transformation is applied:

$$[M]([K] - \sigma_i[M])^{-1}[M]\{\phi_i\} = \theta_i[M]\{\phi_i\}$$

where σ_i is the shift, θ_i is the eigenvalue of the transformed problem and $\{\phi_i\}$ is again the eigenvector. This transformation allows rapid convergence to the desired eigenvalues. The eigenvectors of original and transformed problem are same and the two eigenvalues are related as:

$$\omega_i^2 = \frac{1}{\theta_i} + \sigma_i$$

A Lanczos run is terminated when its continuation is estimated to be inefficient.

Problem Statement

Study of the effect of retrofitting of GFRP sheets for flexure on a simply supported beam in terms of static analysis and frequency analysis with the help of ANSYS Workbench and to develop trends based on the observations and relations between the effect of retrofitting and the configuration of beam.

Verification of Analysis

A standard beam with predefined loading pattern as shown in Fig. 3a is chosen with reinforcement details as shown in Fig. 3b. This beam is 4100 mm in length and is simply supported having a cross section of 127 mm × 227 mm. The supports are at a distance of 3750 mm, which is the effective span of the beam. The beam has 2–10 mmφ Fe 250 bars in the tension side and 2–8 mmφ bars in the compression side. Shear stirrups of 6 mmφ are provided at a distance of 150 mm c/c. M 20 concrete is used as the primary material for beam. This beam is solved

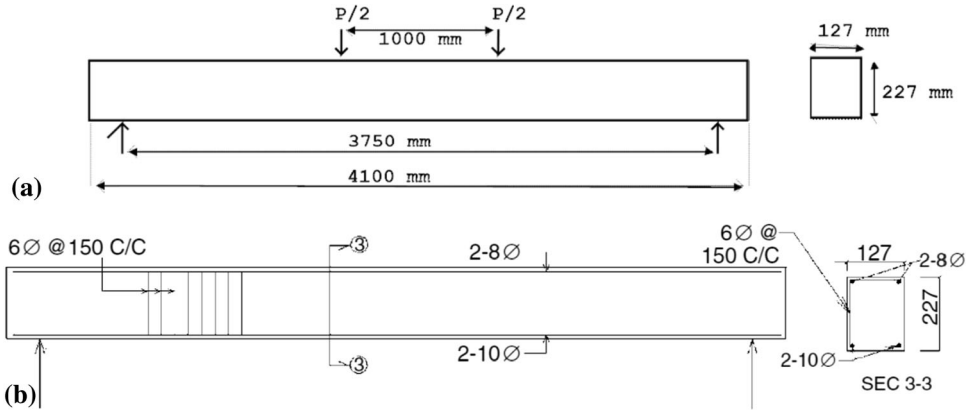

Fig. 3 (**a**) loading arrangement. (**b**) Longitudinal and transverse sections

analytically for a value of load P = 13.3 kN by the methods mentioned in "Verification of analysis" section and then analyzed in ANSYS to obtain the value of deflection at midpoint in both cases.

For the beam in Fig. 3: $E_c = 3 \times 10^4$ Nmm^{-2}

$I_u = 1.341 \times 10^8$ mm^4

The value of flexural rigidity E_cI_u in the transformed area approach is obtained to be 4.0235E + 12 Nmm^2 and the deflection v as a function of span comes out to be:

$$E_cI_uv = -0.1417x^4 + 5.98 \times 10^9x - 1.046 \times 10^{12} + 1108.33\{x - 175^3 - x - 1550^3 - x - 2550^3 + x - 3925^3\}$$

This equation gives the deflection at midpoint as $v_{x=2050} = 3.945$ mm. Analyzing the same beam in ANSYS as shown in Fig. 4a gives the displacement at the midpoint to be 3.653 mm. Support used in the simulation is a prism with a (40 * 40) mm^2 cross section with chamfer of 19 mm on both top edges Fig. 4b and the load bearing block used in the simulation is a semicircular prism of radius 40 mm as shown in Fig. 4c. This process completes with an error of approximately 7%. Hence, it can be concluded that the simulation of the benchmark beam is correct. The same settings, i.e., geometrical setup, meshing and analysis settings, etc. can be used to analyze further cases.

Different Cases of Beams

After the analysis methodology was verified, different cases of beams are generated (approximately 90 in numbers). These beams are very similar to the benchmark beams except variation in the following criteria:

- Aspect ratio (b/d)
- Percentage of steel (P)
- Uniformly distributed loading intensity (w)
- Number of layers of GFRP used

The beams are so chosen that these variations are exclusive of each other, i.e., only one property of the four varies at a time from the benchmark beam.

The GFRP sheets used are of 1 mm thickness and their material is Epoxy S-Glass UD. The variations in beams in this category range from without GFRP to triple layers of GFRP retrofitting. These sheets were bonded to the beam in such a way that the major principal axis of the fibers makes an angle of 45° [14] with the length of the beam as shown in Fig. 5. This ensures maximum effective use of the GFRP retrofitting.

Analysis in ANSYS

The analysis in ANSYS Workbench includes static structural analysis and modal analysis (frequency analysis) as covered in the "Different cases of beams" section. The static analysis is used to generate results for total deformations (e.g., Fig. 6a), equivalent von-Mises strains, equivalent von-Mises stresses and total strain energies. For modal analysis, 5 modes of vibrations are extracted and their natural frequencies and total deformations (Fig. 6b) for Mode IV) are obtained with the different mode shapes.

Results

The variation of static deflection, stress, strain energy, frequency and deflection of various modes with respect to aspect ratio, percentage of steel and loading intensity are discussed in "Verification of analysis", "Different cases of beams and Analysis in ANSYS".

Parametric Study of Beams with Different Aspect Ratio (b/d)

The non-dimensional deflection, tensile stress and total strain energy have been observed in Fig. 7a, b, and c, to increase with the aspect ratio of the beams. However, the

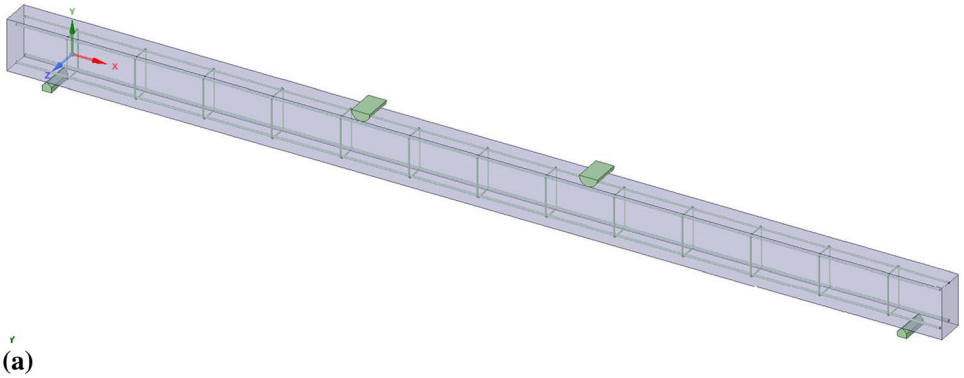

(a)

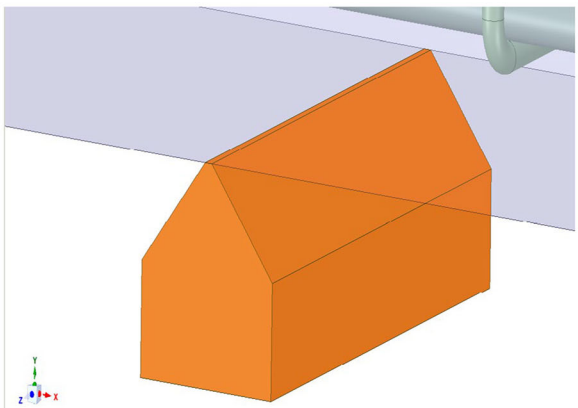

(b)

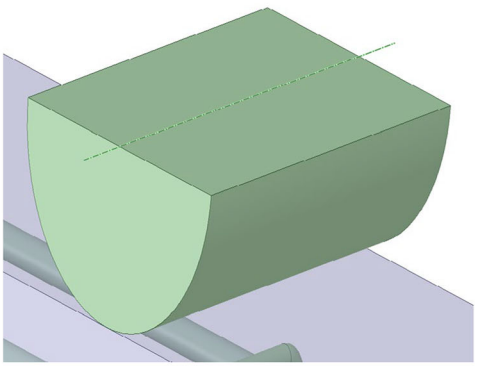

(c)

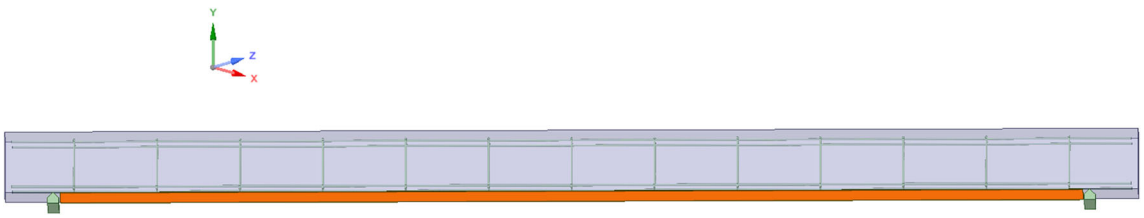

Fig. 4 (**a**) Model of simulated beam, (**b**) Support used in the simulation, (**c**) Load bearing block used in the simulation

Fig. 5 GFRP layer (orange) bonded at the bottom of the beam (Color figure online)

rate of increase is significantly larger for the case of without GFRP and single layer GFRP. The maximum reduction in deflection, stress and strain energy is observed in case of triple layer GFRP at the maximum aspect ratio of the dataset.

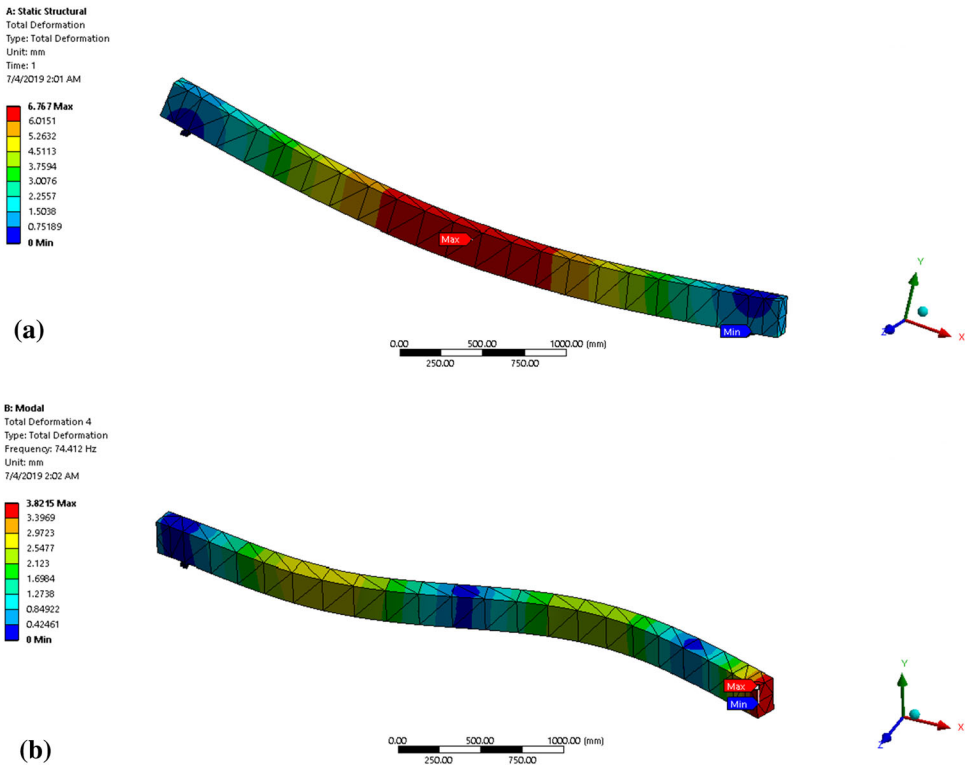

Fig. 6 (**a**) Static structural analysis for total deformation of a beam. (**b**) Modal analysis for mode shape and total deformation of Mode IV of a beam

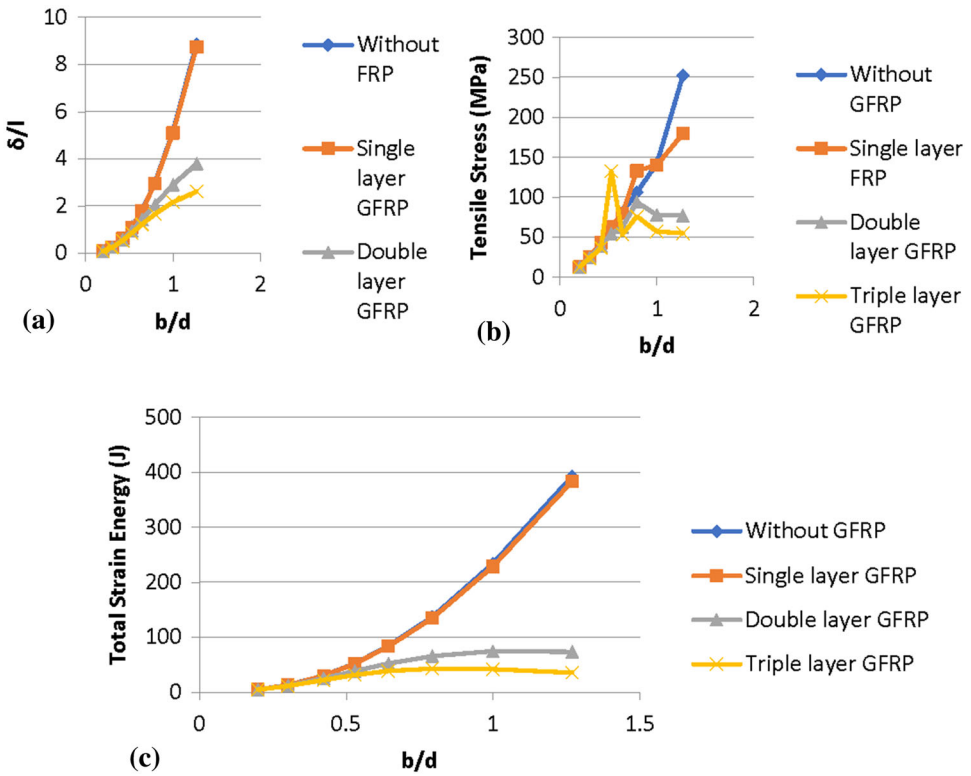

Fig. 7 (**a**) Variation of non-dimensional deflection with respect to aspect ratio. (**b**) Variation of tensile stress with respect to aspect ratio. (**c**) Variation of total strain energy with respect to aspect ratio

Variation of Frequency with Respect to Aspect Ratio for Different Modes

The variation of frequency with respect to the aspect ratio as shown in Fig. 8a, b, c, d, and e, are not monotonous for any mode except Mode I. However, as the number of layers of GFRP increases to three the curves tend to become smooth even achieving monotonous increase in Mode II and IV and a monotonous decrease in Mode III for the case of triple layer GFRP. For Mode V, a local maxima is observed for all cases when the aspect ratio is around 0.5. The increase in frequency between the cases of without GFRP and triple layer GFRP for Mode II is the highest at the maximum aspect ratio of the dataset.

Variation of Deflection with respect to Aspect Ratio for Different Modes

The variation of deflection due to vibration with respect to aspect ratio as shown in Fig. 9a, b, c, d, and e are most consistent for Mode I showing an increase with the aspect ratio for all cases. For Mode II, III and IV, the variations are inconsistent. The case of triple layer GFRP experiences the maximum deflection for some aspect ratio in Mode II and IV while for Mode III and V, it is the single layer GFRP experiencing the maximum deflection for some aspect ratios. Failure due to de-bonding is observed in Mode V at lower aspect ratios thus rendering the deflections to go off charts.

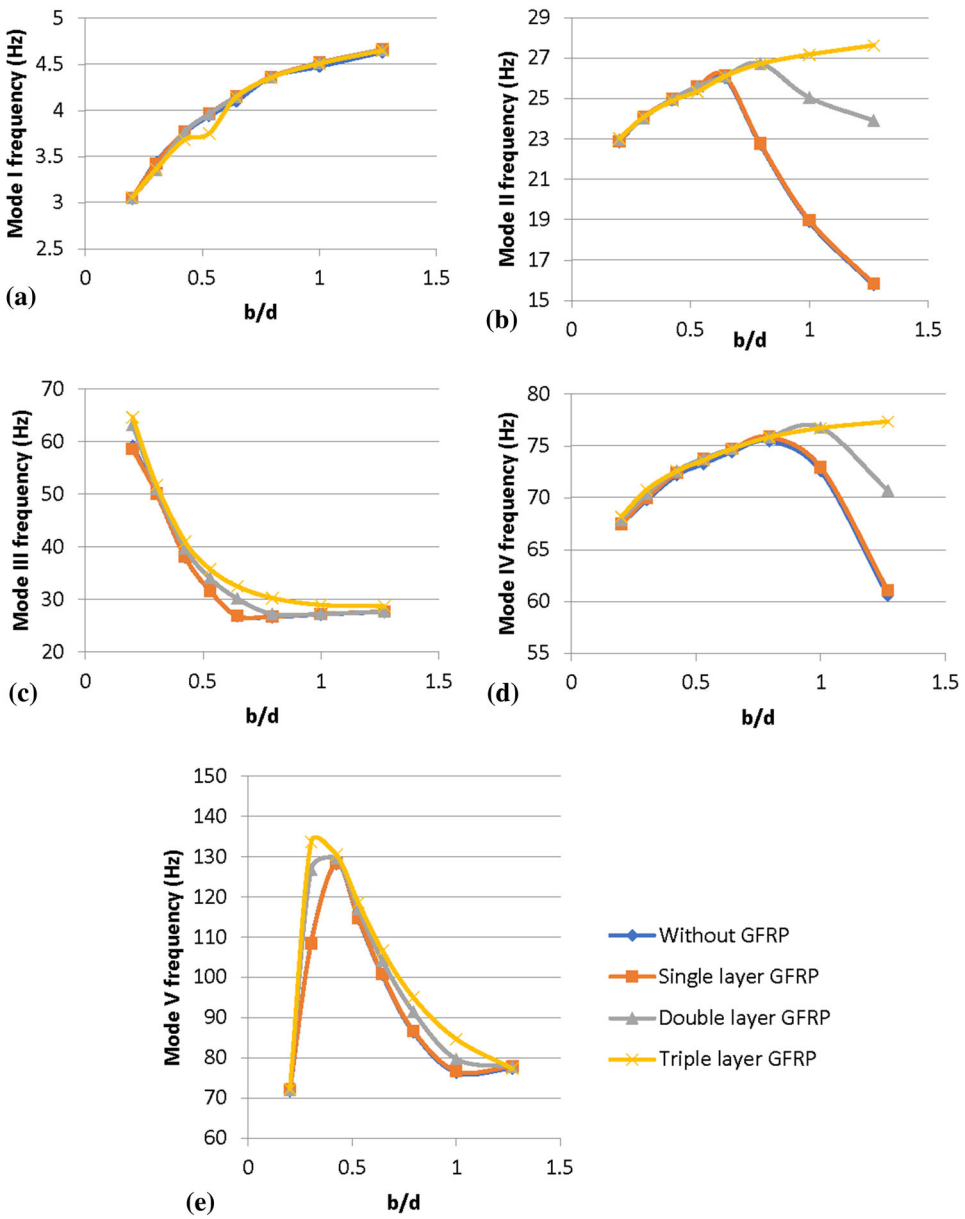

Fig. 8 (**a**) Variation of Mode I frequency with respect to aspect ratio. (**b**) Variation of Mode II frequency with respect to aspect ratio. (**c**) Variation of Mode III frequency with respect to aspect ratio. (**d**) Variation of Mode IV frequency with respect to aspect ratio. (**e**) Variation of Mode V frequencies with aspect ratio

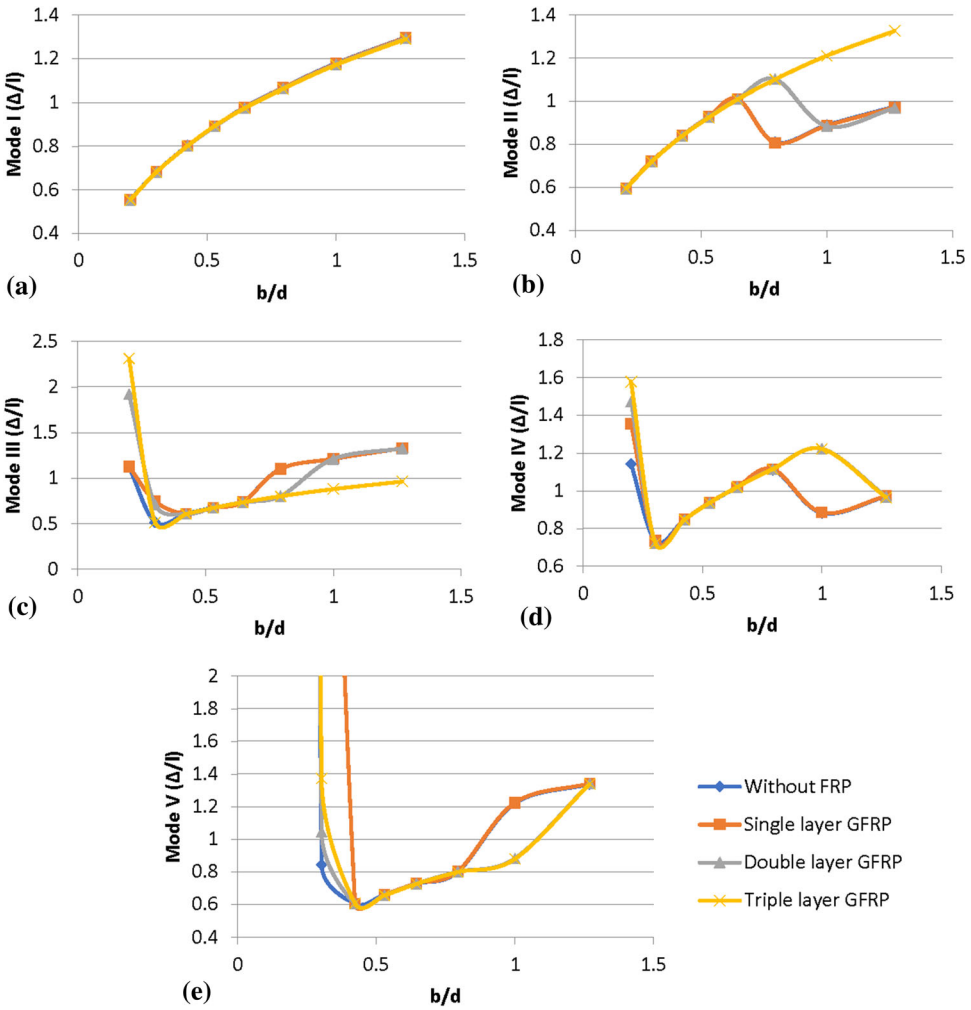

Fig. 9 (**a**) Variation of Mode I deflection with aspect ratio. (**b**) Variation of Mode II deflection with aspect ratio. (**c**) Variation of Mode III deflection with aspect ratio. (**d**) Variation of Mode IV deflection with aspect ratio. (**e**) Variation of Mode V deflections with aspect ratio

Parametric Study of Beams with Different Percentage of Steel (*P%*)

The non-dimensional deflection and total strain energy as shown in Fig. 10a, b, and c are showing a gradual but steady decline with the increase in the percentage of steel. The tensile stresses remain uniform throughout with any number of layers of GFRP. Without GFRP the tensile stresses are inconsistent and have an ultimate rise with the highest percentage of steel in the dataset. Overall, the non-dimensional deflection, tensile stress and total strain energy are minimum and significantly lesser for the case of triple layer GFRP.

Variation of Frequency with Respect to Percentage of Steel for Different Modes

The variation of frequency with respect to (w.r.t.) percentage of steel as shown in Fig. 11a, b, c, d, and e, are very similar for the cases in which retrofitting is done. The behavior of beams without GFRP is significantly different from the other cases which have so much similarity that even their curves are almost same for Mode I, II and IV. For Mode III and V, the variations are similar for all cases and experience a monotonous increase in frequency with significant difference in frequencies of all the cases. There is a local maximum in Mode I, II and IV at 1.6% of steel. For these modes, the retrofitted beams have almost equal frequencies.

Variation of Deflection with Respect to Percentage of Steel for Different Modes

Deflection due to natural vibrations varies the most consistently with percentage of steel out of all the parametric studies performed as can be observed from Fig. 12a, b, c, d, and e. The behaviors of retrofitted beams show a similar result which is slightly different than beam without GFRP in Mode I, II and IV. The deflection in every mode decreases with an increase in the percentage of steel. While in Mode I and II the decrease is not linear, Mode III has almost linear decrease and Mode IV and V experience a

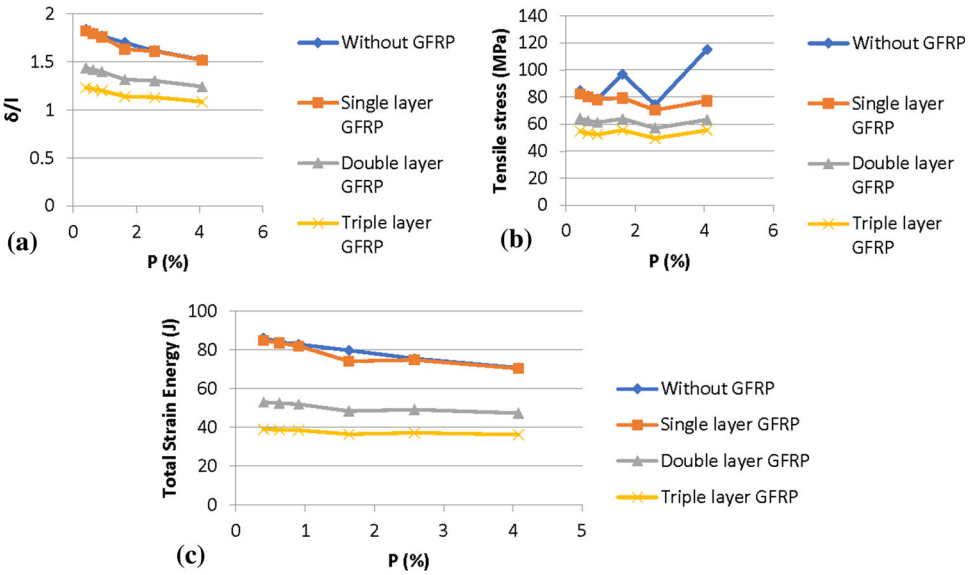

Fig. 10 (**a**) Variation of non-dimensional deflection w.r.t.% of steel. (**b**) Variation of tensile stress with respect to % of steel. (**c**) Variation of Total strain energy with respect to Percentage of steel

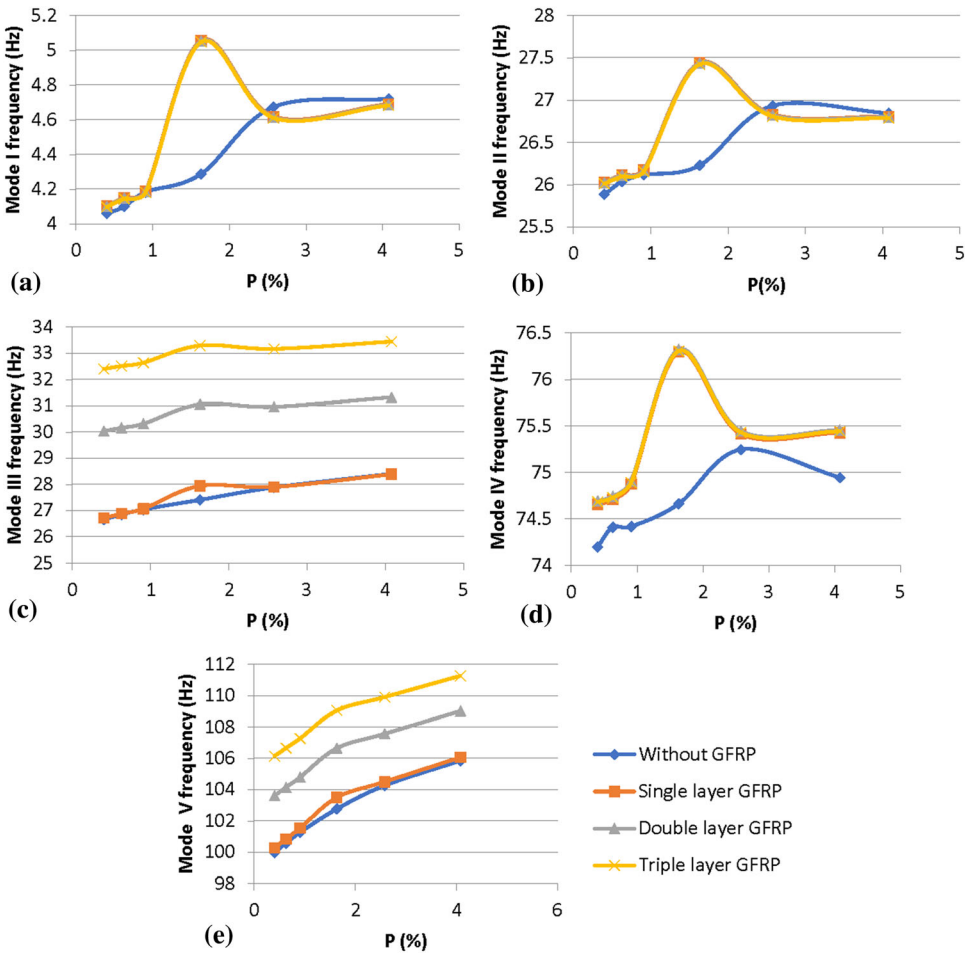

Fig. 11 (**a**) Variation of Mode I frequency w.r.t. Percentage of steel. (**b**) Variation of Mode II frequency w.r.t. Percentage of steel. (**c**) Variation of Mode III frequency w.r.t. percentage of steel. (**d**) Variation of Mode IV frequency w.r.t. Percentage of steel. (**e**) Variation of Mode V frequency w.r.t. Percentage of steel

linear, monotonous decrease in the deflections. For all cases it is observed the deflection is the minimum for triple layer GFRP with exception of a few points where beams without retrofitting have the minimum deflection.

Parametric of Beams with Different Uniformly Distributed Loading Intensities (w)

The non-dimensional deflection and tensile stress are showing a linear increase with respect to the loading intensity while the total strain energy is showing a

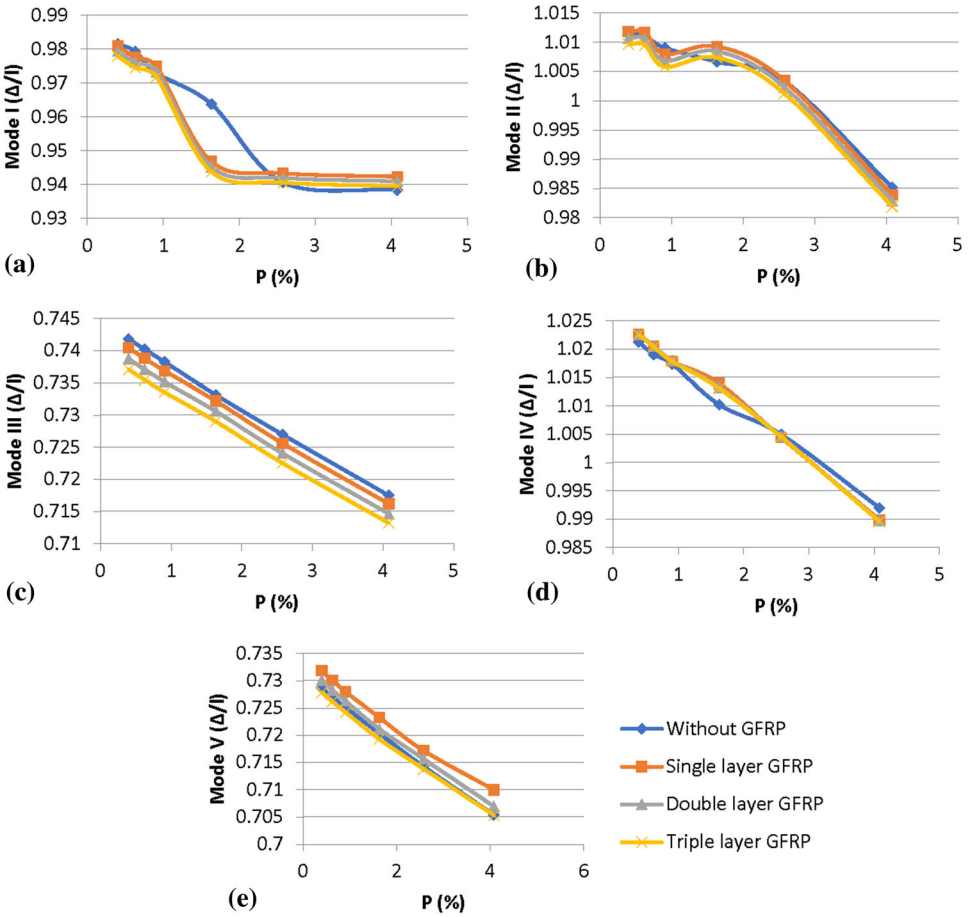

Fig. 12 (**a**) Variation of Mode I deflection w.r.t. Percentage of steel. (**b**) Variation of Mode II deflection w.r.t. Percentage of steel. (**c**) Variation of Mode III deflection w.r.t. Percentage of steel. (**d**) Variation of Mode IV deflection w.r.t. Percentage of steel. (**e**) Variation of Mode V deflection w.r.t. Percentage of steel

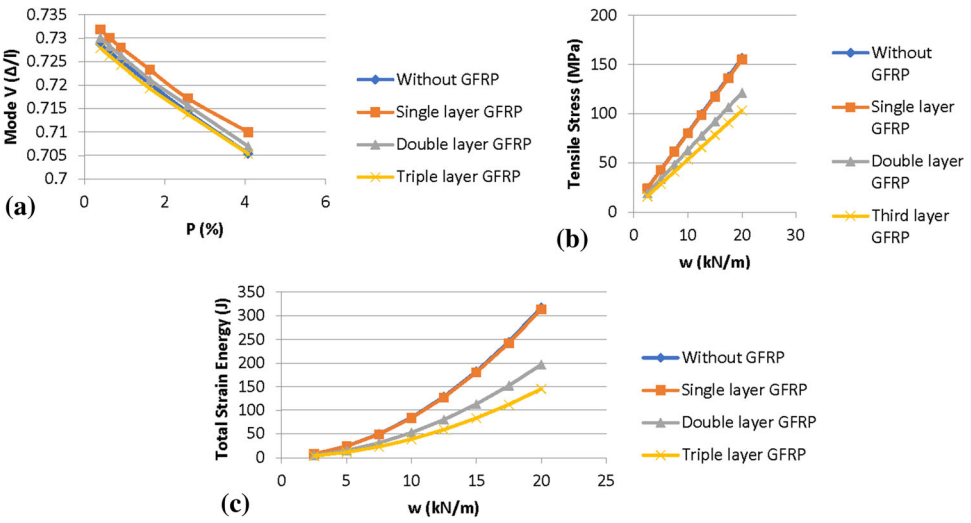

Fig. 13 (**a**) Variation of Non-dimensional deflection w.r.t loading intensity. (**b**) Variation of Tensile w.r.t loading intensity. (**c**) Variation of Total strain energy with respect to loading intensity

quadratic increase as can be observed in Fig. 13a, b, and c. Similar to the earlier studies the beams without GFRP and those with a single layer of GFRP are having almost similar values of deflection, stress and strain energy at different points. The triple layer GFRP is the most effective in reducing the deflection, stress and strain energies at every value of loading intensity. The reduction is maximum at higher loading intensities (91% reduction at w = 20 kN/m).

Variation of Frequency with Respect to Loading Intensity for Different Modes

The frequencies do not appear to vary much with the loading intensity as can be seen in Fig. 14a, b, c, d, and e. For Mode I and II, the frequency decreases slightly with an increase in the loading intensity. For Mode III, this decrease is more subtle. For other modes, the frequency remains constant. There is no particular case which experiences the maximum or minimum frequency values across all modes but overall, it can be implied that frequency may increase slightly with number of layers of GFRP. Except for Mode III, the frequencies of the extreme cases do not vary by more than 6% (Mode IV).

Variation of Deflection with Respect Loading Intensity for Different Modes

Similar to the variations observed in Fig. 15a, b, c, d, and e, deflections due to natural vibrations do not appear to vary much with the loading intensity. For Mode II and III, the deflections are constant. For Mode I, the deflection curves have a gradual upward slope but the increase is not very significant. For Mode IV, the deflection for some cases increase while for some cases it decreases uniformly implying no particular trend. For Mode 5, the deflections are approximately equal and constant for all loading intensities.

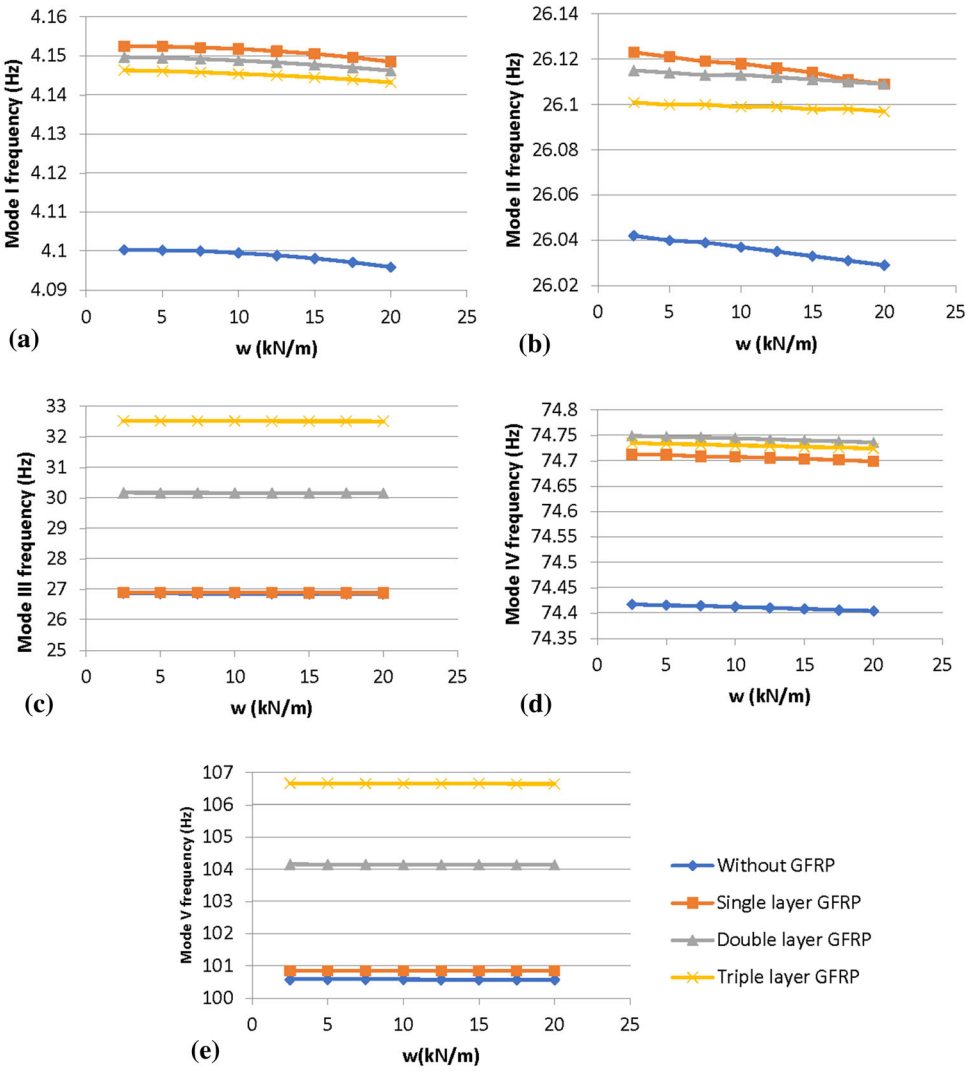

Fig. 14 (**a**) Variation of Mode I frequency w.r.t. loading intensity. (**b**) Variation of Mode II frequency w.r.t. loading intensity. (**c**) Variation of Mode III frequency w.r.t. loading intensity. (**d**) Variation of Mode IV frequency w.r.t. loading intensity. (**e**) Variation of Mode V frequency w.r.t. loading intensity

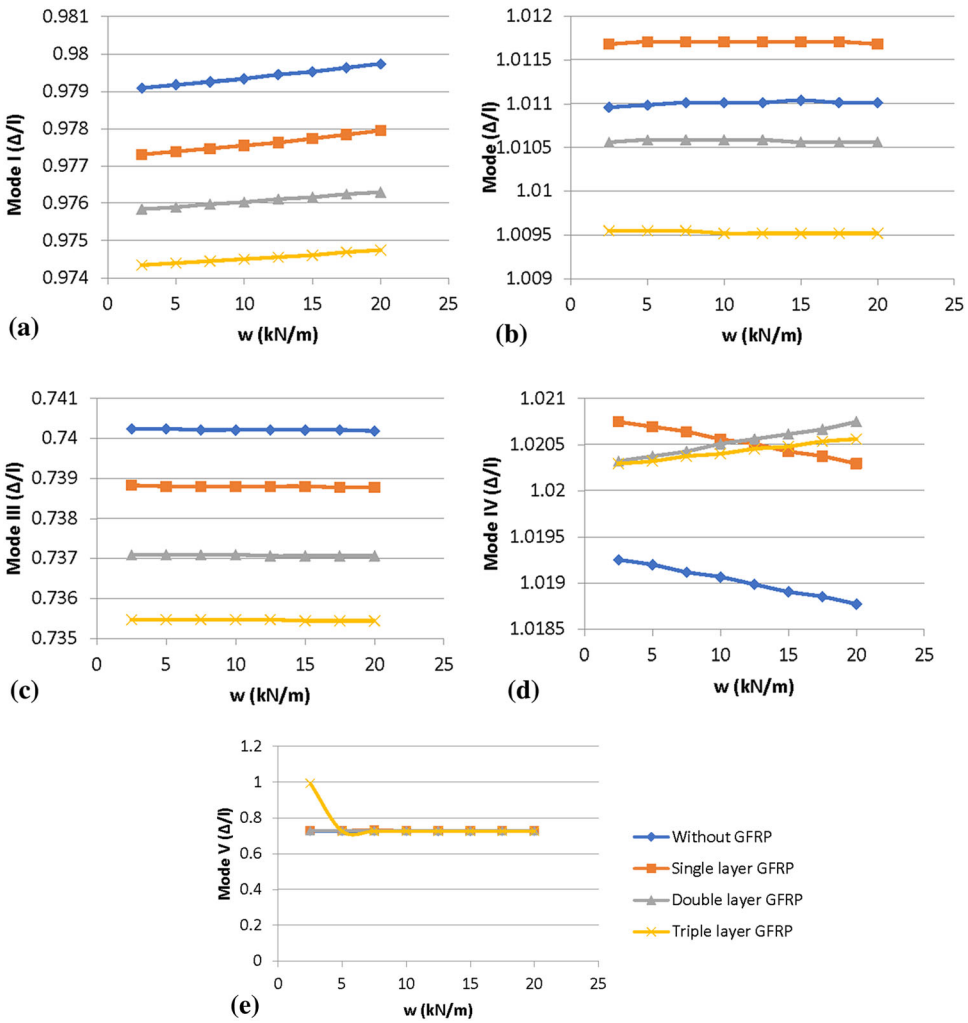

Fig. 15 (**a**) Variation of Mode I deflection w.r.t. loading intensity. (**b**) Variation of Mode II deflection w.r.t. loading intensity. (**c**) Variation of Mode III deflection w.r.t. loading intensity. (**d**) Variation of Mode IV deflection w.r.t. loading intensity. (**e**) Variation of Mode V deflection w.r.t. loading intensity

Regression Analysis

The process mentioned above generates a large array of data and these data are then used in Microsoft Excel to develop relations between the reduction in deflections, stresses, strain energies, increase in strength, change in natural frequencies, etc. and the configuration of beam with the extent of retrofitting. For this purpose, a multivariate polynomial regression analysis is done with polynomials up to fourth degree in case of frequency analysis and up to third degree in case of static analysis.

The data obtained from the simulation of different cases are used to obtain the relation between various parameters for different layers of retrofitting. The developed equations are listed in this section

Relations for Beam Without GFRP

$$\frac{\delta}{l} = -1.445 + 0.169w - 0.213P + 0.0165P^3 - 1.893m + 7.009m^3 - 0.0206m^3;$$
$$r^2 = 0.999$$

$$\sigma = -124.074 + 7.585w - 10.955P + 4.07P^2 + 362.99m - 390.031m^2 + 231.046m^3;$$
$$r^2 = 0.989$$

$$E = -72.744 + 1.012w + 0.742w^2 - 9.855P + 0.723P^2 - 88.448m + 341.64m^2 - 22.579m^3;$$
$$r^2 = 0.999$$

$$v = -11.822 + 4.659n^2 - 0.135n^3 + 0.613P + 96.103m - 163.203m^2 + 70.774m^3;$$
$$r^2 = 0.941$$

Relations for Beam with Single Layer GFRP

$$\text{Reduction in } \frac{\delta}{l}(\%) = -0.196 + 8.729P - 4.013P^2 + 0.512P^3 - 0.6785m + 2.889m^2; \quad r^2 = 0.502$$

$$\text{Reduction in } \sigma(\%) = 32.521 + 43.097P - 20.465P^2 + 3.227P^3 + 178.266m - 379.194m^2 + 204.44m^3; \quad r^2 = 0.713$$

$$\text{Reduction in } E(\%) = -0.326 + 15.025P - 6.922P^2 + 0.884P^3 - 11.265m + 4.637m^2; \quad r^2 = 0.497$$

Relations for Beam with Double Layer GFRP

$$\text{Reduction in } \frac{\delta}{l}(\%) = 1.165 + 3.272P - 2.197P^2 + 0.292P^3 - 21.726m + 108.409m^2 - 45.153m^3; \quad r^2 = 0.999$$

$$\text{Reduction in } \sigma(\%) = -17.498 + 31.032P - 15.952P^2 + 2.584P^3 + 77.42m - 103.447m^2 + 66.916m^3; \quad r^2 = 0.896$$

$$\text{Reduction in } E(\%) = -2.923 + 3.913P - 2.847P^2 + 0.378P^3 - 4.375m + 149.458m^2 - 74.583m^3; \quad r^2 = 0.998$$

Relations for Beam with Triple Layer GFRP

$$\text{Reduction in } \frac{\delta}{l}(\%) = -1.281 + 0.114w - 0.1086P + 0.0107P^2 + 0.398m + 4.15m^2 - 2.119m^3; \quad r^2 = 0.999$$

$$\text{Reduction in } \sigma(\%) = -12.005 + 25.417P - 13.717P^2 + 2.252P^3 + 45.342m + 10.769m^2; \quad r^2 = 0.934$$

$$\text{Reduction in } E(\%) = -16.036 - 1.044P^2 + 0.1346P^3 + 82.711m + 81.052m^2 - 62.537m^3; \quad r^2 = 0.997$$

where $\frac{\delta}{l}$ = Non-dimensional deflection due to static loading, i.e., deflection to span ratio, σ = Tensile stress in bars (MPa), E = Total strain energy (J), n = Number of mode of vibration, v = Natural frequency (Hz), w = Uniformly distributed loading intensity (kN/m), P = Percentage of steel (%), $m = \frac{b}{d}$ = Aspect ratio, i.e., width to effective depth ratio, $\frac{\Delta}{l}$ = Non-dimensional deflection due to natural vibration, i.e., deflection to span ratio.

Conclusions

From the study it can be concluded that the effect of GFRP retrofitting on the reduction in deflection and stress and the increase in strength is positive. However, the same cannot be said about the increase in natural frequency of vibrations with such certainty. As suspected, the triple layer setup is found to be the most effective with up to 70% reduction in deflection, 78% reduction in tensile stress and 91% reduction in case of total strain energy (Fig. 7).

In the case of frequency most of the cases show an increase in frequency even up to 75% (Fig. 8b) with increase in layers of GFRP but there also are non-negligible numbers of discrepancies showing a decrease of up to 2.3%. Here, an absolute trend is not established but since the increase is comparatively very large than the decrease, it can be said that there is overall an increase of natural frequencies across all modes with an increase in number of layers of GFRP. The case of deflection of natural mode of vibration is very uncertain and trends for this case are not well established. The deflections for different modes do not appear to follow any particular trend as studied in different parametric studies. However, the most consistent results for this case are observed in variations with respect to the percentage of steel which clearly shows that the deflection decreases with increase in the number of GFRP layers.

The regression analysis resulted in very accurate relations for static deflection, stress, strain energy and natural frequency for different layers. The relative percentage decrease in all these quantities except frequency are also quantified as equations quite accurately but for the case of frequency the relations developed were not accurate and hence discarded.

It can also be concluded that single layer of GFRP does not have any significant change on the concerned quantities of deflection, stress, etc., but for noticeable effects double and triple layers of GFRP are suitable, with the best results being achieved by the triple layer GFRP setup.

References

1. Z. Saleh, M.N. Sheikh, A.M. Remennikov, A. Basu, Numerical investigations on the flexural behavior of GFRP-RC beams under monotonic loads. Structures **20**, 255–267 (2019). https://doi.org/10.1016/j.istruc.2019.04.004
2. H. Soltani, A. Khaloo, H. Sadraie, Dynamic performance enhancement of RC slabs by steel fibers vs. externally bonded

GFRP sheets under impact loading. Eng. Struct. **213**, 110539 (2020). https://doi.org/10.1016/j.engstruct.2020.110539
3. A.K. Shukla, P.R. Maiti, G. Rai, Retrofitting of damage rail bridge girder and its performance evaluation. J. Fail. Anal. Prev. (2020). https://doi.org/10.1007/s11668-020-00890-1
4. A.K. Shukla, P.R. Maiti, Retrofitting and rehabilitation of damage footbridge over yamuna river. Int. J. Recent. Technol. Eng. **8**, 4239–4246 (2019). https://doi.org/10.35940/ijrte.B2667.078219
5. E. Esmaeeli, F. Danesh, K.F. Tee, S. Eshghi, A combination of GFRP sheets and steel cage for seismic strengthening of shear-deficient corner RC beam-column joints. Compos. Struct. **159**, 206–219 (2017). https://doi.org/10.1016/j.compstruct.2016.09.064
6. R. Capozucca, E. Magagnini, M.V. Vecchietti, Damaged RC beams strengthened with GFRP. Procedia Struct. Integr. **11**, 402–409 (2018). https://doi.org/10.1016/j.prostr.2018.11.052
7. P.P. Bansal, M. Kumar, SK Kaushik "Experimental study on retrofitting of stressed RC beam using GFRP jackets". J. Reinf. Plast. Compos. **29**(2), 190–200 (2008)
8. Wu Yu-Fei, Tao Lio, Deric J. Oehlers, Fundamental principles that govern retrofitting of reinforced concrete columns by steel and FRP jacketing. Adv. Struct. Eng. **9**(4), 507–533 (2006)
9. K.C. Chang, S.P. Chang, Seismic retrofit study of rectangular RC columns lap spliced at plastic hinge zone. Proc. Joint NSC/NRC Workshop on Constr. Technol. **2004**, 27–34 (2004)
10. Xian Li, Heng-Lin Lv, Guang-Chang Zhang, Shi-Yu. Sha, S.-C. Zhou, Seismic retrofitting of reinforced concrete columns using fiber composites for enhanced flexural strength. J. Reinf. Plast. Compos. **32**(9), 619–630 (2013)
11. Alper Ilki, Cem Demir, Idris Bedirhanoglu, N. Kumbasar, Seismic retrofit of brittle and low strength RC columns using fiber reinforced polymer and cementitious composites. Adv. Struct. Eng. **12**(3), 325–347 (2009)
12. H.S. Birajdar, P.R. Maiti, P.K. Singh, Failure of chauras bridge. Eng. Fail. Anal. **45**, 339–346 (2014). https://doi.org/10.1016/j.engfailanal.2014.06.015
13. K.M. Mahmood, S.A. Ashour, S.I. Al-Noury, Effective moment of inertia and deflections of reinforced concrete beams under long term loading. Eng. J. Univ. Qatar **8**, 101–125 (1995)
14. J.M. Gere, B.J. Goodno, Mechanics of material. Cengage Learn. 479–485 (2012), ISBN-13: 978-1-111-13602-4